The X-Ray Source at the Center of the Cassiopeia A Supernova Remnant

Mereghetti, S.; Tiengo, A.; Israel, G.L.

Published in:
Astrophysical Journal

DOI:
10.1086/339277

The Astrophysical Journal, 569:275–279, 2002 April 10

THE X-RAY SOURCE AT THE CENTER OF THE CASSIOPEIA A SUPERNOVA REMNANT

S. Mereghetti
Istituto di Fisica Cosmica G. Occhialini-CNR, via Bassini 15, I-20133 Milan, Italy; sandro@ifctr.mi.cnr.it

A. Tiengo
XMM-Newton Science Operation Center VILSPA ESA, Apartado 50727, 28080 Madrid, Spain; tiengo@xmm.vilspa.esa.es

and

G. L. Israel
Osservatorio Astronomico di Roma, via Frascati 33, I-00040 Monteporzio Catone, Italy; gianluca@mporzio.astro.it
Received 2001 September 5; accepted 2001 December 19

ABSTRACT

We present the first results of an *XMM-Newton* observation of the central X-ray source in the Cas A supernova remnant. The spectrum can be fitted equally well with an absorbed steep power law ($\alpha_{\rm ph} \sim 3$, $N_{\rm H} \sim 1.5 \times 10^{22}$ cm^{-2}) or with a bremsstrahlung with temperature $kT \sim 2.4$ keV and $N_{\rm H} \sim 10^{22}$ cm^{-2}. A blackbody model ($kT_{\rm BB} \sim 0.7$ keV) gives a slightly worse fit and requires a column density $N_{\rm H} \sim 5 \times 10^{21}$ cm^{-2} and an emitting area with radius $\sim$0.3 km (for $d = 3.4$ kpc). A search for pulsations for periods longer than 150 ms gave negative results. The 3 σ upper limits on the pulsed fraction are $\sim$13% for $P > 0.3$ s and $\sim$7% for $P > 3$ s. The overall properties of the central X-ray source in Cas A are difficult to explain in terms of a rapidly spinning neutron star with a canonical magnetic field of $\sim 10^{12}$ G, and are more similar to those of slowly rotating neutron stars such as the anomalous X-ray pulsars.

Subject headings: stars: neutron — supernovae: individual (Cassiopeia A) — X-rays: stars

1. INTRODUCTION

The long-sought compact remnant born in the Cas A supernova explosion was discovered in the first-light image obtained with the *Chandra* X-ray satellite (Tananbaum 1999). For the following reasons, there is little doubt that CXO J232327.8+584842 (CXO for brevity) is indeed associated with Cas A, the youngest ($\sim$320 yr) supernova remnant observed in the Galaxy (Ashworth 1980; Fesen et al. 1987).

First, the X-ray flux of $\sim 10^{-12}$ ergs cm^{-2} s^{-1} (Pavlov et al. 2000; Chakrabarty et al. 2001) and the strong upper limits on any optical/IR counterpart in the small (1″ radius) *Chandra* error circle ($R > 26.3$, $K > 21.2$; Ryan et al. 2001; Kaplan et al. 2001) imply for CXO an X-ray–to–optical flux ratio greater than $\sim$800. This immediately excludes any kind of noncompact Galactic source as well as accreting binary systems, unless the companion star is a very low mass object. On the other hand, the X-ray–to–optical flux ratio of CXO is similar to that of radio pulsars and other neutron star candidates (see, e.g., Shearer & Golden 2001; Treves et al. 2000).

Second, CXO is located at an angular distance $\lesssim 7''$ from the site of the Cas A supernova explosion, which has been recently redetermined with good accuracy by a backward projection of the expanding optical filaments (Thorstensen et al. 2001). For an age of 320 yr and a distance of 3.4 kpc (Reed et al. 1995), the implied transverse speed of the neutron star would be $\sim$340 km s^{-1}, well within the range of the observed space velocities of radio pulsars (Cordes & Chernoff 1998).

Finally, the possibility of a background extragalactic source has been dismissed (Pavlov et al. 2000) on the basis of (1) the very small probability of finding an active galactic nucleus (AGN) as bright as CXO within an area of only $\sim$0.05 arcmin^2, and (2) the steep power-law X-ray spectrum of CXO.

Although the association with Cas A is well established, the exact nature of CXO remains puzzling. Deep radio observations (McLaughlin et al. 2001) were unable to detect any source, either pulsed (upper limit of 1.3 mJy at 1.4 GHz) or unpulsed (upper limit of 40 and 6 mJy at 1.3 and 4.4 GHz, respectively). A radio/X-ray synchrotron nebula could indicate the presence of a rapidly rotating, magnetized neutron star, even when beam orientation effects prevent its direct observation as a radio pulsar. However, no radio or X-ray (Murray et al. 2002) nebula has been found around CXO.

The X-ray spectrum of CXO is not well constrained. Equally good fits to the *Chandra* data were obtained with simple power-law, blackbody, and bremsstrahlung models (Pavlov et al. 2000; Chakrabarty et al. 2001; Murray et al. 2002). Power-law fits give a steep photon index $\alpha_{\rm ph} \sim 3$–4 and a column density $N_{\rm H} \sim (1.5$–$2.3) \times 10^{22}$ cm^{-2}, larger than the estimated value of the interstellar absorption in the direction of Cas A (Keohane et al. 1996). Young neutron stars emitting in the X-ray band by nonthermal magnetospheric processes have harder spectra ($\alpha_{\rm ph} \sim 1.5$) and higher luminosity ($L_{\rm X} \sim 10^{35}$–10^{36} ergs s^{-1}) than CXO. The fits with a blackbody model give $kT_{\rm BB} \sim 0.5$ keV and $N_{\rm H} \sim 10^{22}$ cm^{-2}, but they imply an emitting area that, for any reasonable assumed distance, is far too small to be consistent with the surface of a neutron star. This discrepancy is not uncommon when fitting cooling neutron stars with simple blackbody spectra. Larger emitting areas, more consistent with the neutron star dimensions, are generally obtained when more appropriate models for the thermal emission from neutron star atmospheres are used (see, e.g., Zavlin et al. 1998, 1999). However, Pavlov et al. (2000) showed that in the case of Cas A, even fits with neutron star atmosphere models imply emission from only a small fraction of the star surface.

A reanalysis of archival *Einstein* and *ROSAT* observations showed no evidence for long-term variability (Pavlov et al. 2000). Searches for X-ray pulsations have been carried out with *Chandra* by Chakrabarty et al. (2001) with negative results, and later by Murray et al. (2002), who reported a possible periodicity at 12 ms, but with a very low statistical significance. If this period were confirmed, it would be difficult to explain the lack of a strong pulsar wind nebula around CXO, unless its magnetic field is rather low ($\lesssim 5 \times 10^{10}$ G).

Here we report the results of an observation of CXO performed with the *XMM-Newton* satellite on 2000 July 27 as part of the performance verification program.

2. OBSERVATIONS

The data reported here were obtained with the European Photon Imaging Camera (EPIC) instrument on the *XMM-Newton* satellite. EPIC consists of two MOS CCD detectors (Turner et al. 2001) and a PN CCD instrument (Strüder et al. 2001), giving a total collecting area $\gtrsim$2500 cm^2 at 1.5 keV. The mirror system offers an on-axis FWHM angular resolution of 4″–5″ and a field of view of 30′ diameter.

The *XMM-Newton* observation of Cas A started at 6:45 UT on 2000 July 27 and lasted about 11 hr. The telemetry saturation due to the high overall counting rate from the supernova remnant caused a noncontinuous operation of the CCDs, yielding effective exposures of 9219 s in the PN, and 23573 and 23594 s in the MOS1 and MOS2 detectors, respectively. The satellite was pointed at the center of the remnant (R.A.: $23^h23^m25^s$, decl: 58°48′20″ [J2000]), resulting in the detection of CXO very close to the center of the EPIC field of view (off-axis angle of 0.′52). During this observation the thin filter was used. The MOS cameras were operated in "large window" mode to limit the source photon pile-up. The background-corrected count rates of CXO were 0.25 ± 0.02 and 0.13 ± 0.01 counts s^{-1} in the PN and in each MOS, respectively.

The data were analyzed with version 5.2 of the *XMM-Newton* Science Analysis System. The counts for the spectral analysis were extracted in the three EPIC cameras from circles with 10″ radii centered at the *Chandra* position of CXO. Such a small radius, enclosing only about 50% of the counts from a point source, was chosen to avoid contamination from bright nearby filaments because of the emission from the supernova remnant (see the *Chandra* images of Murray et al. 2002 and Chakrabarty et al. 2001). All the spectral fits reported below were obtained with the appropriate response matrices that take into account the dimensions of the extraction region. The derived fluxes are corrected for the fraction of counts outside the 10″ circle.

CXO is relatively faint compared to the nonuniform, diffuse emission due to Cas A. We estimate that the background accounts for ~75%–80% of the counts within the adopted extraction radius (14,050 for the PN and 13,320 for the MOS1). Therefore, we devoted particular attention to the choice of the region for the extraction of the background spectra. Based on the high-resolution *Chandra* images, we tried different regions with a surface brightness similar to that at the position of CXO and avoided bright filaments. We found that the resulting CXO spectra are somewhat dependent on the chosen background that can lead to the presence of residuals near the energies of the strongest Cas A emission lines. Such residuals in the background-subtracted spectra were minimized using the background from a rectangular (~20″ × 15″) region to the east of CXO, roughly corresponding to the eastern half of that used in the *Chandra* analysis by Chakrabarty et al. (2001). The spectra discussed below were obtained with this choice of the background region.

For the PN spectra we used photons corresponding to single and double events, after checking that the individual single- and double-event spectra gave the same results within the uncertainties. The energy channels were grouped to have at least 30 net counts per bin, and the fits were performed in the 0.6–10 keV energy range. The results of power-law, blackbody, and bremsstrahlung fits are summarized in Table 1.

The same extraction and binning criteria were applied to the two MOS cameras. While the results obtained with MOS1 agree with the PN results (see Table 1), the MOS2 fits gave different parameters and worse χ^2 values. We found that this discrepancy is due to the fact that at the time of the *XMM-Newton* observation of Cas A, the offset calculation for the MOS cameras was still based on an imperfect onboard algorithm (only later in the mission were better fixed tables implemented). This problem can cause spurious event detections in channels close to the low-energy threshold, and it also produces an offset of the energy scale in particular regions of the CCD. By carefully examining the MOS2 image and comparing spectra of different regions, we verified that in this observation such an effect occurred just at the position of CXO in the MOS2. Since these effects cannot be easily corrected, we did not consider the MOS2 spectra in our further analysis.

To better constrain the spectral parameters, we jointly fitted the PN and MOS1 data (Table 1). The power-law and bremsstrahlung models give better fits to the data, while the fit with a blackbody (Fig. 1) yields higher χ^2 values. For comparison with the results of Murray et al. (2002), we also present in Table 1 the values obtained by fixing $N_H = 1.1 \times 10^{22}$ cm^{-2} and by adding a power law to the blackbody model. For all the models, the observed 0.1–10 keV flux from the joint PN-MOS1 fits is of the order of $\sim 2 \times 10^{-12}$ erg cm^{-2} s^{-1}. The systematic difference between the PN and MOS1 fluxes must be ascribed to the uncertainties in the relative calibration of the two detectors. The errors on the luminosities reported in Table 1 have been

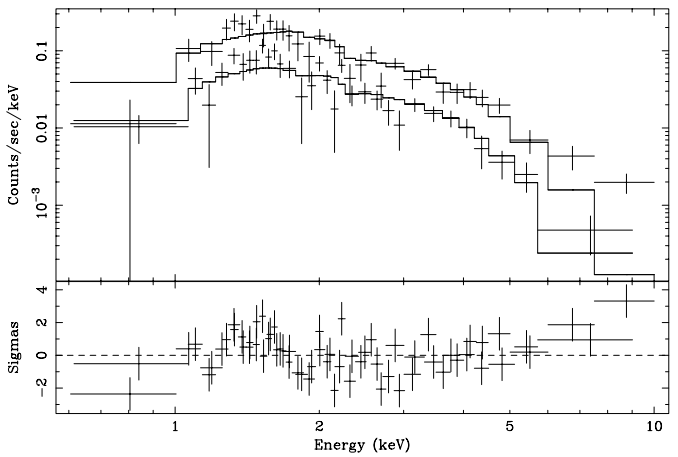

FIG. 1.—EPIC PN and MOS1 spectra of CXO fitted with a blackbody model.

TABLE 1
RESULTS OF SPECTRAL FITS

Model	N_H[a] (10^{22} cm^{-2})	α_{ph}[a]	kT[a] (keV)	Flux[b] (10^{-12} ergs s^{-1} cm^{-2})	L_X[c] (10^{33} ergs s^{-1})	χ^2_{red}/dof
			PN			
Power law	$1.47^{+0.34}_{-0.27}$	$2.85^{+0.31}_{-0.27}$	...	2.3	51^{+101}_{-25}	1.09/30
Blackbody.....	$0.46^{+0.19}_{-0.15}$	...	0.75 ± 0.06	2.0	3.5 ± 0.3	1.63/30
Bremsstrahlung.....	$1.04^{+0.23}_{-0.18}$	...	$2.64^{+0.65}_{-0.50}$	2.2	$8.0^{+1.9}_{-1.3}$	1.13/30
			MOS1			
Power law	$1.53^{+0.42}_{-0.33}$	$3.16^{+0.46}_{-0.39}$	...	1.9	92^{+364}_{-69}	1.04/29
Blackbody.....	$0.47^{+0.18}_{-0.17}$	...	0.65 ± 0.07	1.67	$3.1^{+0.5}_{-0.3}$	1.27/29
Bremsstrahlung.....	$1.06^{+0.27}_{-0.13}$	...	$1.98^{+0.60}_{-0.42}$	1.8	$8.2^{+3.5}_{-2.0}$	1.03/29
			PN + MOS1			
Power law	$1.47^{+0.25}_{-0.21}$	$2.96^{+0.25}_{-0.23}$	...	2.1	60^{+63}_{-29}	1.07/61
Blackbody.....	$0.46^{+0.14}_{-0.12}$	...	0.70 ± 0.05	1.8	$3.2^{+0.3}_{-0.2}$	1.49/61
Bremsstrahlung.....	$1.03^{+0.17}_{-0.14}$	...	$2.36^{+0.44}_{-0.36}$	2.0	$7.9^{+1.5}_{-1.2}$	1.11/61
Power law	1.1 (fixed)	2.60 ± 0.11	...	2.1	$24.3^{+5.5}_{-4.3}$	1.20/62
Blackbody.....	1.1 (fixed)	...	0.60 ± 0.03	1.7	$4.2^{+0.1}_{-0.1}$	2.00/62
PL + BB.....	1.1 (fixed)	$2.62^{+0.33}_{-0.32}$	$0.62^{+0.18}_{-0.12}$	2.1	$19.5^{+22.8}_{-9.9}$	1.09/60

[a] Errors at 90% confidence level for a single interesting parameter.
[b] Absorbed flux 0.1–10 keV.
[c] 0.1–10 keV luminosity ($d = 3.4$ kpc) corrected for absorption.

computed taking into account the uncertainties of the spectral parameters and absorption (90% c.l. for two interesting parameters).

For the timing analysis, we extracted all the counts with energy in the 1–6 keV energy range from circles with radius 10″ centered on the CXO position. This yielded 12,276, 12,652, and 12,511 counts for the PN, MOS1, and MOS2 detectors, respectively. The upper limits reported below take into account that the background, estimated from nearby regions, accounts for ~75% of these counts. After correction of the arrival times to the solar system barycenter, a Fourier analysis of the background-subtracted light curves was performed using the method described in Israel & Stella (1996). The frequency resolution was 2.46×10^{-5} Hz. The frame integration times of 0.073 and 0.9 s in the PN and MOS cameras, respectively, set the upper limits to the explored frequency ranges. No significant periodicity was found. The upper limits on the pulsed fraction, computed according to Vaughan et al. (1994), are shown in Figure 2 as a function of the frequency. The curves refer to the 3 σ upper limit on the source-pulsed fraction in the 1–6 keV energy range assuming a sinusoidal modulation. Above 0.4 Hz only the PN data could be used, while at lower frequencies we could sum the power spectra from the three instruments, thus improving the sensitivity, as shown by the lower curve of Figure 2. Also, separate searches in the soft (1–2 keV) and hard (2–6 keV) energy ranges gave negative results. The corresponding upper limits are about a factor of 2 higher than those shown in Figure 2.

3. DISCUSSION

Our spectral results can be compared with those derived from the *Chandra* observations. In the power-law case, our best-fit values for α_{ph} and N_H are consistent with the values found by Chakrabarty et al. (2001), but not with the more recent findings of Murray et al. (2002), who obtain a softer and more absorbed spectrum. The temperature values that we find for the bremsstrahlung and blackbody models are higher than the *Chandra* values, and the corresponding column densities slightly smaller. The blackbody normalization of our fits implies an emitting area with radius of $0.32 d_{3.4\ \mathrm{kpc}}$ km, smaller than that inferred with *Chandra*. To check whether the discrepancy with respect to the *Chandra* results might be explained by the higher background contribution in the EPIC spectral extraction region, we also performed an analysis with smaller source extraction regions, down to a radius of 5″ (always using the appropriate response matrices). The derived best-fit parameters did not vary significantly.

The above-mentioned difficulties in interpreting the X-ray emission from CXO in terms of a young active pulsar are therefore confirmed by our *XMM-Newton* results. An independent knowledge of the expected column density could help to discriminate among the various spectral mod-

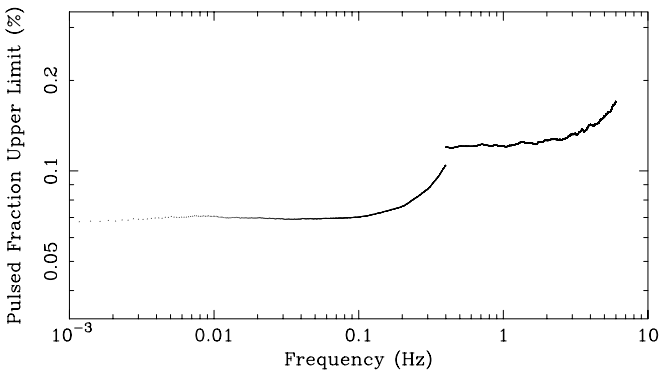

FIG. 2.—Upper limits (3 σ) on the CXO pulsed fraction (semiamplitude of a sinusoidal modulation after background subtraction). The curve for $\nu < 0.4$ Hz was obtained from the sum of MOS1, MOS2, and PN data, while at higher frequencies only the PN data could be used.

els. Values in the range $(0.9–1.3) \times 10^{22}$ cm^{-2} have been derived by Keohane et al. (1996), with significant variations across the remnant and with relatively smaller absorption at the position of CXO. On this basis, the thermal bremsstrahlung fit is the one giving the most consistent N_H value. The low absorption, as well as the higher χ^2 value, suggests that the simple blackbody fit is not adequate. The trend of the residuals shown in the lower panel of Figure 1 (see also Fig. 3 of Murray et al. 2002) probably indicates that atmosphere models more complex than simple blackbody spectra are required.

The soft spectrum and high X-ray–to–optical flux ratio make CXO similar to the anomalous X-ray pulsars (AXPs; Mereghetti 2001a). These objects have periods in the 6–12 s range, steadily increasing on timescales of $\sim 10^3$–10^5 yr, and two (possibly three) of them are located at the center of shell-like supernova remnants. Similar properties (except for the periodicity) are shared by the X-ray sources at the center of the supernova remnants Puppis A (Petre et al. 1996; Zavlin et al. 1999), G290.5+10.0 (Mereghetti et al. 1996; Zavlin et al. 1998), RCW 103 (Gotthelf et al. 1999), and G266.1−1.2 (Slane et al. 2001; Mereghetti 2001b; Pavlov et al. 2001b). The bolometric blackbody luminosity and temperature of all these sources are plotted in Figure 3, where for comparison we have also included two classes of older neutron stars: three middle-aged radio pulsars from which thermal emission from internal cooling has been observed (PSR B1055−52, PSR B0656+14, and Geminga; see, e.g., Becker & Trümper 1997) and several nearby isolated neutron stars (Treves et al. 2000 and references therein). For all the sources in which a nonthermal spectral component is also present, we have plotted in Figure 3 only the bolometric luminosity of the blackbody component.

The AXPs have on average a higher luminosity than the central compact objects (CCOs) in supernova remnants, but their blackbody temperatures are very similar. Although the majority of AXPs and CCOs have quite stable luminosity, there are two interesting variable sources that might be

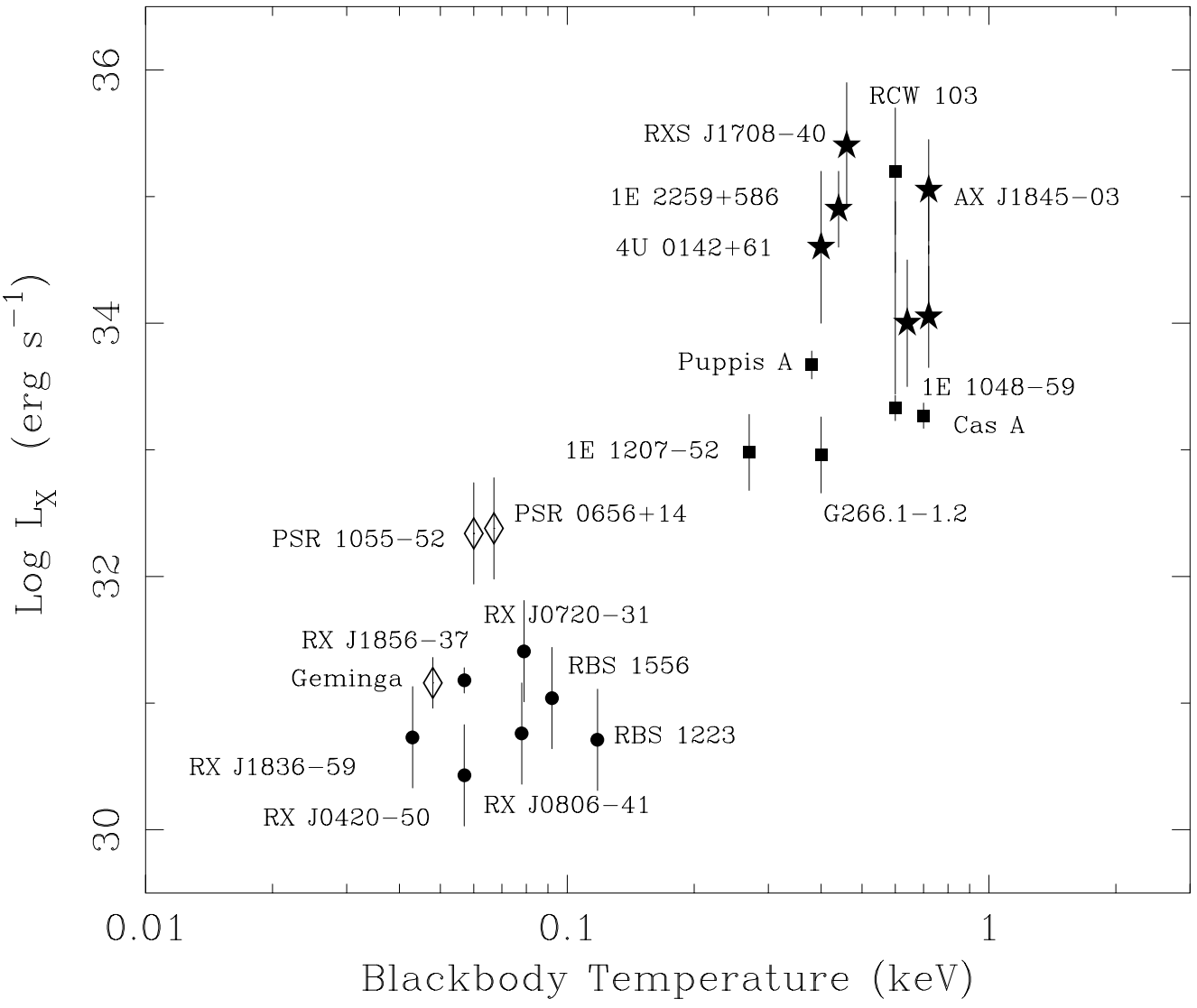

FIG. 3.—" Color-magnitude " diagram for different classes of neutron stars: AXPs (*stars*), supernova remnant CCOs (*squares*), nearby isolated neutron stars (*circles*), and radio pulsars (*diamonds*). For the luminosity of AXP and radio pulsars, only the thermal spectral component is considered. To allow the comparison between the different objects, we plotted the temperatures inferred from pure blackbody fits; the use of atmosphere models would move all the points to lower temperatures by a factor of ∼2–3. The luminosity error bars reflect the distance uncertainties. The two positions for RCW 103 and AX J1845−03 indicate the observed variability range.

intermediate objects linking these two classes. The candidate AXP AX J1845−03 has been observed since 1997 at a flux level corresponding to $L_X \lesssim 10^{34}$ ergs s^{-1} (Torii et al. 1998; Vasisht et al. 2000), at least 10 times smaller than at the time of its discovery. 1E 1614−5055, the CCO in RCW 103, already known to be variable between $F_{0.5-2\,keV} \sim 3$ and $\sim 50 \times 10^{-13}$ erg cm^{-2} s^{-1} (Gotthelf et al. 1999) and with a possible ~6 hr periodicity (Garmire et al. 2000a), has recently been detected with *Chandra* in an even higher state (Garmire et al. 2000b).

Alpar (2001) proposed a unified interpretation of the classes of objects shown in Figure 3, in which they are all assumed to be neutron stars with ordinary magnetic fields (10^{11}–10^{13} G), thus avoiding the need for supercritical magnetic fields required by the "magnetar" models for AXPs (e.g., Thompson & Duncan 1996). According to Alpar (2001), isolated neutron stars experience a mass inflow due to the formation of a residual accretion disk from fallback material after the supernova explosion. This causes an evolutionary phase in the propeller regime, before the neutron star turns on as a radio pulsar or as an AXP, depending on the initial conditions in terms of rotational period, magnetic field, and mass in the residual disk (see also Chatterjee et al. 2000 for a similar model). The dim, nearby neutron stars in the lower left corner of Figure 3 are interpreted as examples of sources in the propeller regime, in which the X-ray emission is from cooling powered by internal friction. The CCOs would be the propeller objects with the highest mass inflow, surrounded by an optically thick corona, and might evolve into AXPs (Alpar 2001).

Searches for periodicities in the CCOs extending to low frequencies are therefore relevant, since some of these objects might have periods similar to those of the AXP. In this respect, we note that, while the CCO in G290.5+10.0 has a fast period of 424 ms (Zavlin et al. 2000) and might be a "radio-quiet" pulsar similar to Geminga, the fast periodicity at 75 ms reported in the Puppis A CCO (Pavlov et al. 1999) has not been confirmed by more accurate *Chandra* observations (Pavlov et al. 2001a). For frequencies $\nu < 6$ Hz, our limits on the pulsed fraction of CXO are smaller than those previously obtained with *Chandra* (Chakrabarty et al. 2001; Murray et al. 2002). Only one of the AXPs has a pulsed fraction as small as 7% (see, e.g., Israel et al. 2002), our upper limit for long periods.

4. CONCLUSIONS

We have reported the first results of an *XMM-Newton* observation of CXO, the interesting X-ray point source at the center of the Cas A supernova remnant. The large collecting area of the *XMM-Newton* instruments has allowed us to derive strong upper limits of ~13% for $P > 0.3$ s and ~7% for $P > 3$ s on the pulsed fraction (3 σ).

The spectral analysis confirmed the very soft spectrum of CXO, but yields, in the case of thermal models, higher temperatures than those measured earlier with *Chandra*. The source luminosity does not show evidence of long-term variations when compared with previous measurements.

As for other candidate neutron stars in supernova remnants older than Cas A, the overall properties of CXO are difficult to explain in terms of a rapidly spinning neutron star with a canonical magnetic field of $\sim 10^{12}$ G, and are more similar to those of slowly rotating neutron stars such as the AXPs.

We acknowledge the financial support of the Italian Space Agency. This work is based on observations obtained with *XMM-Newton*, an ESA science mission with instruments and contributions directly funded by ESA member states and NASA.

REFERENCES

Alpar, A. 2001, ApJ, 554, 1245
Ashworth, W. B. 1980, J. Hist. Astron., 11, 1
Becker, W., & Trümper, J. 1997, A&A, 326, 682
Chakrabarty, D., et al. 2001, ApJ, 548, 800
Chatterjee, P., Hernquist, L., & Narayan, R. 2000, ApJ, 534, 373
Cordes, J. M., & Chernoff, D. F. 1998, ApJ, 505, 315
Fesen, R. A., Becker, R. H., & Blair, W. P. 1987, ApJ, 313, 378
Garmire, G., et al. 2000a, IAU Circ. 7350
———. 2000b, BAAS, 32, 32.11
Gotthelf, E. V., Petre, R., & Vasisht, G. 1999, ApJ, 514, L107
Israel, G. L., Mereghetti, S., & Stella, L. 2001, in Proc. Miniworkshop on Soft Gamma Repeaters and Anomalous X-ray Pulsars, ed. M. Feroci & S. Mereghetti (Rome: Mem. Soc. Astron. Italiana), in press (astro-ph/0111093)
Israel, G. L., & Stella, L. 1996, ApJ, 468, 369
Kaplan, D. L., Kulkarni, S. R., & Murray, S. S. 2001, ApJ, 558, 270
Keohane, J. W., Rudnick, L., & Anderson, M. C. 1996, ApJ, 466, 309
McLaughlin, M. A., et al. 2001, ApJ, 547, L41
Mereghetti, S. 2001a, in The Neutron Star–Black Hole Connection, ed. C. Kouveliotou, J. van Paradijs, & J. Ventura (NATO ASI Ser.; Dordrecht: Kluwer), in press (astro-ph/9911252)
———. 2001b, ApJ, 548, L213
Mereghetti, S., Bignami, G. F., & Caraveo, P. 1996, ApJ, 464, 842
Murray, S. S., et al. 2002, ApJ, 566, 1039
Pavlov, G. G., Sanwal, D., Garmire, G. P., & Zavlin, V. E. 2001a, in ASP Conf. Ser., Neutron Stars in Supernova Remnants, ed. P. O. Slane & B. M. Gaensler (San Francisco: ASP), in press (astro-ph/0112322)
Pavlov, G. G., Zavlin, V. E., & Trümper, J. 1999, ApJ, 511, L45
Pavlov, G. G., et al. 2000, ApJ, 531, L53
———. 2001b, ApJ, 559, L131
Petre, R., Becker, C. M., & Winkler, P. F. 1996, ApJ, 465, L43
Reed, J. E., et al. 1995, ApJ, 440, 706
Ryan, E., Wagner, R. M., & Starrfield, S. G. 2001, ApJ, 548, 811
Shearer, A., & Golden, A. 2001, ApJ, 547, 967
Slane, P., et al. 2001, ApJ, 548, 814
Strüder, L., et al. 2001, A&A, 365, L18
Tananbaum, H. 1999, IAU Circ. 7246
Thompson, C., & Duncan, R. C. 1996, ApJ, 473, 322
Thorstensen, J. R., Fesen, R. A., & van den Bergh, S. 2001, AJ, 122, 297
Torii, K., et al. 1998, ApJ, 503, 843
Treves, A., Turolla, R., Zane, S., & Colpi, M. 2000, PASP, 112, 297
Turner, M. J. L., et al. 2001, A&A, 365, L27
Vasisht, G., Gotthelf, E. V., Torii, K., & Gaensler, B. M. 2000, ApJ, 542, L49
Vaughan, B. A., et al. 1994, ApJ, 435, 362
Zavlin, V. E., Pavlov, G. G., Sanwal, D., & Trümper, J. 2000, ApJ, 540, L25
Zavlin, V. E., Pavlov, G. G., & Trümper, J. 1998, A&A, 331, 821
Zavlin, V. E., Trümper, J., & Pavlov, G. G. 1999, ApJ, 525, 959